JOTCS B
Journal of the Turkish Chemical Society
Section: B
Chemical Engineering
TURKISH CHEMICAL SOCIETY

Preparation of Waste Fabric Based Activated Carbon and Determination of Adsorption Performance Using Methylene Blue

Yavuz Gokce

[1]Ankara University, Department of Chemical Engineering, Ankara, 06100, Turkey

Abstract: The acceleration of industrialisation and population growth throughout the world have caused the rapid depletion of water resources in the last century. Industrial wastes are one of the major factors causing water pollution. One of the most effective and well-known methods to prevent water pollution is adsorption process. In this study, highly porous activated carbons were produced using waste fabric samples and their adsorption performances were determined in the presence an adsorbate to prevent water pollution. Methylene blue (MB) as the adsorbate was used for the adsorption tests. The waste fabric samples were carbonised at 400 °C, 500 °C and 600 °C to determine the effect of pre-carbonisation temperature on the adsorption performance. The activated carbon surface properties varied depending on the pre-carbonisation temperature. The surface areas of the samples were 1385 m^2/g, 1583 m^2/g and 1276 m^2/g, and the total pore volumes were 0.7688 cm^3/g, 0.9545 cm^3/g and 0.7394 cm^3/g, respectively. The results showed that the pre-carbonisation temperature affected the adsorption performance. The adsorption capacities of the activated carbons calculated according to the Langmuir adsorption model were 531.46 mg/g, 630.26 mg/g and 655.40 mg/g, respectively.

Keywords: Activated carbon, carbonisation, activation, heat treatment, adsorption

Submitted: September 05, 2023. **Accepted:** September 27, 2023.

Cite this: Gokce, Y. (2023). Preparation of Waste Fabric Based Activated Carbon and Determination of Adsorption Performance Using Methylene Blue. Journal of the Turkish Chemical Society, Section B: Chemical Engineering, 6(2), 85–94. https://doi.org/10.58692/jotcsb.1355600.

***Corresponding author. E-mail:** ygokce@eng.ankara.edu.tr.

1. INTRODUCTION

Water is a crucial substance necessary for all living things in the world to survive. The continuity and diversity of life depend on the existence of water (Shiklomanov, 2000). Developments in the fields of science, technology, and health after the Industrial Revolution have caused radical changes throughout the world. The most important of these is the rapid increase in the world population. The world population, which was 1 billion at the beginning of the 19th century, reached 7.8 billion in 2021 and exceeded 8 billion today, because of the developments in the health sector and the rapid decrease in child mortality rates (Unnerstall, 2022). Due to the increase in population, the amount of water per capita is also decreasing. On the other hand, production amounts are increasing in every sector due to industrialisation. The increase in production naturally leads to an increase in the amount of industrial waste generated. Industrial wastes are one of the important factors that have negative effects on water pollution (Shukla et al., 2002). Therefore, protecting all water resources, especially drinking and utility water, keeping them clean and cleaning contaminated water resources are vital for the sustainability of life. Methods for cleaning contaminated water are generally grouped under six main processes: adsorption, biotechnology, catalytic, membrane, ionising radiation, and magnetically assisted processes (Ambashta & Sillanpää, 2010). These methods have various advantages and disadvantages compared to each other. The process of cleaning contaminated water by adsorption is the most preferred among them (Chai et al., 2021). Thousands of studies on this topic are published in literature every year.

In the process of water purification, contaminants in water are retained on the surface of a solid (adsorbent) by adsorption. There are many factors that affect the amount of contaminant that can be adsorbed on the solid surface. Many studies are frequently conducted on many parameters such as the amount of solid, the surface chemistry of the solid, the physical properties of the solid such as particle size and surface area, the molecular size of

the adsorbate, temperature, mixing, ambient pH value (Bushra et al., 2021; Rápó & Tonk, 2021). The characteristics (physical and chemical) of the adsorbent are the most important factors that affect the adsorption performance. It is possible to find studies using many different adsorbents such as clay (Bentchikou et al., 2017), biomass (Darama et al., 2022), activated carbon (Gokce et al., 2021), metal oxide (Ayranpınar et al., 2023), metal organic lattice structures (Wang et al., 2021), carbon nanotube (Avcı et al., 2020), graphene (Yang & Cao, 2022). The low price and easy accessibility of the raw material from which the adsorbent is obtained is the reason for economic preference as it will reduce the cost of the adsorption process. Materials such as clay and biomass are very economical materials since they are found spontaneously in nature, but the adsorption capacity of such adsorbents is not at the expected level. Activated carbons are materials with very good adsorption performance thanks to their high surface area. They are not found in nature by themselves. However, they can be easily produced from carbon-containing materials such as fossil-based coal (Yaglikci et al., 2021), biomass (Gürten İnal et al., 2020), polymers (Wróbel-Iwaniec et al., 2015). Carbon-containing materials, especially in waste form, reduce the production cost as they are very cheap. For this reason, activated carbons are one of the most preferred materials in the adsorption process. Water treatment systems in which activated carbons are used in industrial or domestic scale are very common in daily life. The adsorption properties of activated carbons come to the fore in sectors such as treatment systems, mining, health, defense industry, energy storage (Gayathiri et al., 2022). Activated carbon has been prepared using various waste biomasses such as coconut shell (Daud & Ali, 2004), bamboo (Liu et al., 2010), hazelnut shell (Ozpinar et al., 2022), tea waste (Gokce & Aktas, 2014), olive kernel (Eder et al., 2021), cumin stalk (Gurten Inal et al., 2018) etc. and their adsorption performances against various pollutants have been tested. Such raw materials make activated carbon production sustainable as they are formed by themselves in tons every year. Another raw material that will enable sustainable activated carbon production even if it does not occur spontaneously in nature is waste textile products. Textile products are produced from carbon-based natural and synthetic fibres. The most commonly used natural fibre source is cotton and synthetic fibre source is polyester. Cotton is composed of cellulose, and cellulose is the most abundant natural polymer in nature.

The amount of production of textile products is increasing in a yearly basis. Especially in the last 200 years, when the population has increased very rapidly, the total amount of textile fibres required for clothing production has also increased rapidly. Annual fibre production is expected to increase further as they are being used in the fields of medicine, construction, automotive, agriculture, packaging, electronics, etc. due to their technical properties. The amount of fibre production, which was around 57 million tons in the 2000s, reached 110 million tons a few years ago (Ütebay et al., 2020). The gradual increase in textile production brings up an important problem such as textile waste. The recycling percentage of textile waste is very low at 25% (Juanga-Labayen et al., 2022). The low recycling percentage significantly affects the sustainability of the textile industry. Although the number of scientific or applied studies on the recycling of textile solid wastes is limited, interest in these wastes has been increasing in recent years (Cao et al., 2022; Pais et al., 2022; Reike et al., 2023; Ütebay et al., 2020). Some applications where new products are used through recycling of textile wastes are as follows; disposable diapers, sanitary napkins, sterile wraps, workwear, wiping cloths, biogas production, dress lining, carpet and upholstery fabrics, wall coverings, car interior and headliner, seat belts, filtration systems, sound insulation materials, reinforced cement, ground reinforcement for roads, building insulation, etc. (Barbero-Barrera et al., 2016; Jeihanipour et al., 2013). In recent years, the production of new garments using recycled fibres has also become increasingly common among brands. Another recycling application of textile wastes is activated carbon production. Some studies on the adsorption performance of activated carbons produced from textile wastes were found in periodicals. However, none of these studies included the impacts of the change in activated carbon surface properties on adsorption performance.

Within the scope of this study, it was intended to produce suitable adsorbent using a waste shirt with 100% cotton fabric content and to investigate the methylene blue adsorption capability of the adsorbent from water. Since it is known that activated carbon surface properties directly affect adsorption performance, different pre-carbonisation temperatures were tried during production. Thus, it was also investigated how the physical and chemical properties of the produced activated carbon samples affect the adsorption performance.

2. EXPERIMENTAL SECTION

2.1. Materials

A 100% cotton shirt that cannot be worn and repaired was used as the waste fabric raw material. Since the selected fabric cannot be used for the purpose of production (wearing), it is considered as waste. Potassium hydroxide (KOH, Merck) was used as activating material in activated carbon production. Methylene blue (MB, Merck) was preferred in adsorption experiments as the adsorbate. No further purification process was performed for the chemicals used.

2.2. Activated Carbon Production

A piece of at least 1 g was cut from the waste shirt, which is cut into smaller pieces and dried in the oven at 105 °C for 12 h. The dried fabric pieces were weighed, and the amount of starting material was determined. Activated carbon production consists of two steps: carbonisation (pre-

carbonisation) in the presence of N_2 (first step) and carbonisation/activation in an inert N_2 atmosphere at a higher temperature (second step). The pre-carbonisation temperature was changed to determine the effects of activated carbons surface properties on adsorption performance. In the pre-carbonisation process, the dried waste fabric samples were transferred to a porcelain crucible and placed in a heat treatment furnace with the lid closed. The furnace was set to the desired pre-carbonisation temperature in N_2 atmosphere for 1 h. The heating rate was 10 °C/min. The furnace was then allowed to cool down to room temperature on its own. The pre-carbonisation temperatures examined in the study were 400 °C, 500 °C and 600 °C. For activated carbon production, the pre-carbonised samples are mixed with KOH so that the ratio of carbonised sample:KOH by weight is 1:3. The appropriate amount of KOH was dissolved in 30 mL of distilled water, carbonised fabric samples were added and mixed for at least 3 h. The mixture was dried at 105 °C for overnight to remove water. After drying, the furnace was set to 800 °C with a heating rate of 10 °C/min and the final carbonisation and activation processes were carried out for 1 h. The final carbonisation and activation temperature was kept constant for all samples. The samples obtained at the end of the process were washed in distilled water and the activation chemical was completely removed. The prepared activated carbon samples were labelled as AC-400, AC-500 and AC-600 according to the pre-carbonisation temperature applied.

2.3. Adsorption Tests

The adsorption performances of the produced samples were determined using MB dye which is frequently used in textiles. Before the adsorption process, a stock MB solution was prepared at a concentration of 500 ppm. Using the stock dye solution, dye solutions of 25 ppm, 50 ppm, 100 ppm, 150 ppm, 200 ppm, 250 ppm, 300 ppm and 350 ppm were prepared in 50 mL volumes. 0.01 g of activated carbon was added to each solution and stirred for 16 h at 30 °C with the help of an orbital shaker (Gerhardt) operating at 150 rpm. After mixing, 10 mL samples of each solution were separated using disposable PTFE filters (0.45 µm).

2.4. Characterisation Studies

Brunauer-Emmett-Teller (BET) surface areas and pore size distributions of activated carbon samples were determined by Quantachrome NOVA 2200 series volumetric gas adsorption system. Non-local density functional theory (NLDFT) was used for pore size distributions. Fourier-Transform Infrared Spectroscopy (FTIR, Shimadzu FTIR-8040) was used for the determination of the surface functional groups present in the structures of the samples. FTIR analysis was performed in the wavenumber range of 4000-400 cm^{-1}. Before the analysis, the AC-400, AC-500 and AC-600 samples were mixed with potassium bromide at a ratio of 1:1200 (activated carbon: potassium bromide) to prepare pellets. Pellet preparation was carried out under vacuum to remove carbon dioxide and moisture that may be trapped in the interparticle spaces and on the particle surface. The wettability properties of the samples were determined by Attension Theta Lite Optical Contact Angle device according to the sessile drop contact angle method. The adsorption capacities of the AC-400, AC-500 and AC-600 samples were determined with the help of a UV-Vis spectrophotometer (Scinco S-3100) at a wavelength of 664 nm where MB has a maximum absorbance.

3. RESULTS AND DISCUSSION

3.1. Specific Surface Area and Pore Size Distribution

The effects of pre-carbonisation temperature on the structural surface properties of the produced activated carbon samples was determined by BET surface area and pore size distribution analysis. N_2 adsorption-desorption isotherms of the samples are given in Figure 1. As can be seen from the figure, the adsorbed N_2 volumes differed for all samples. This result showed that activated carbons had different surface areas. The BET surface area values were calculated using 0.05-0.3 relative pressure (P/P_0) data. The BET surface areas of AC-400, AC-500 and AC-600 samples were 1385 m^2/g, 1583 m^2/g and 1276 m^2/g, respectively. The isotherms were like Type IV isotherms according to the pore classification of the International Union of Pure and Applied Chemistry (IUPAC). The rapid increase of adsorption isotherms at low relative pressure values indicated the presence of micropores in the structure. Also, it was clearly seen from the isotherms that adsorption and desorption curves do not follow the same path and hysteresis occurs. This indicated the presence of mesopores in the structure in addition to micropores.

The pore size distributions are shown in Figure 2. Supporting the results obtained by adsorption-desorption isotherms, all samples had micropore and mesoporous structure simultaneously. AC-500 had the highest surface area and the highest cumulative pore volume. The total pore volume values of AC-400, AC-500 and AC-600 samples were calculated with the help of adsorption isotherms data at 0.99 relative pressure. The total pore volume values were 0.7688 cm^3/g, 0.9545 cm^3/g and 0.7394 cm^3/g, respectively. Structural surface properties of the samples such as the BET surface area, total pore volume, micropore and mesopore volumes, micropore and mesopore fractions were given in Table 1. According to IUPAC, pores smaller than 2 nm were classified as micropores. Micropore volumes were determined using the data obtained by NLDFT method. Mesopore volumes were calculated from the difference between total pore volumes and micropore volumes. As can be deduced from the results, micropore volumes of the samples were higher than mesopore volumes. However, different BET surface areas, pore volumes and pore fractions were formed due to the change in pre-carbonisation temperature.

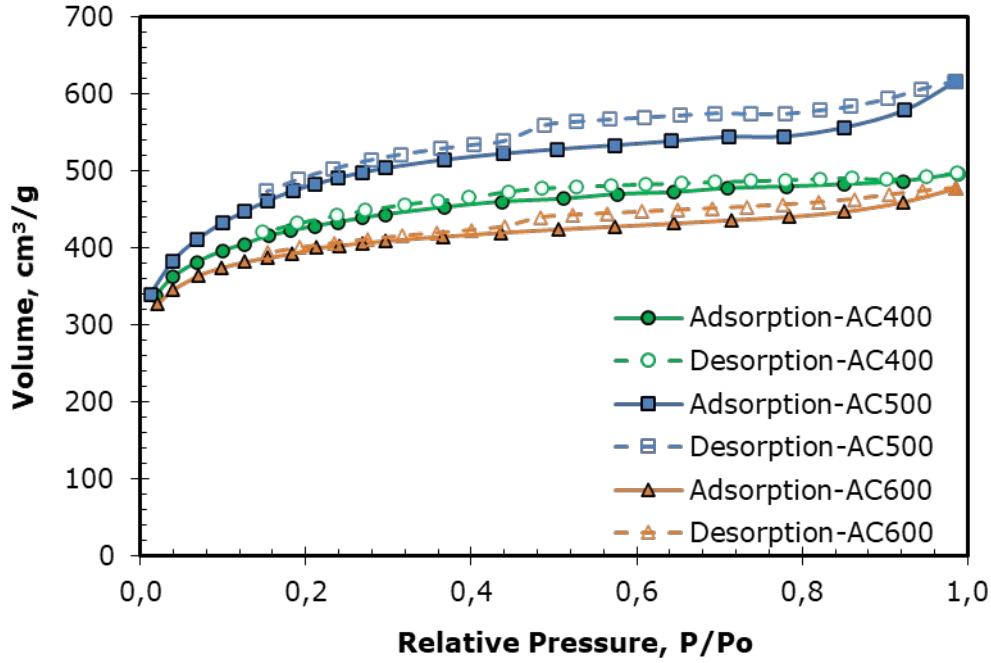

Figure 1: N_2 adsorption-desorption isotherms of AC-400, AC500 and AC-600.

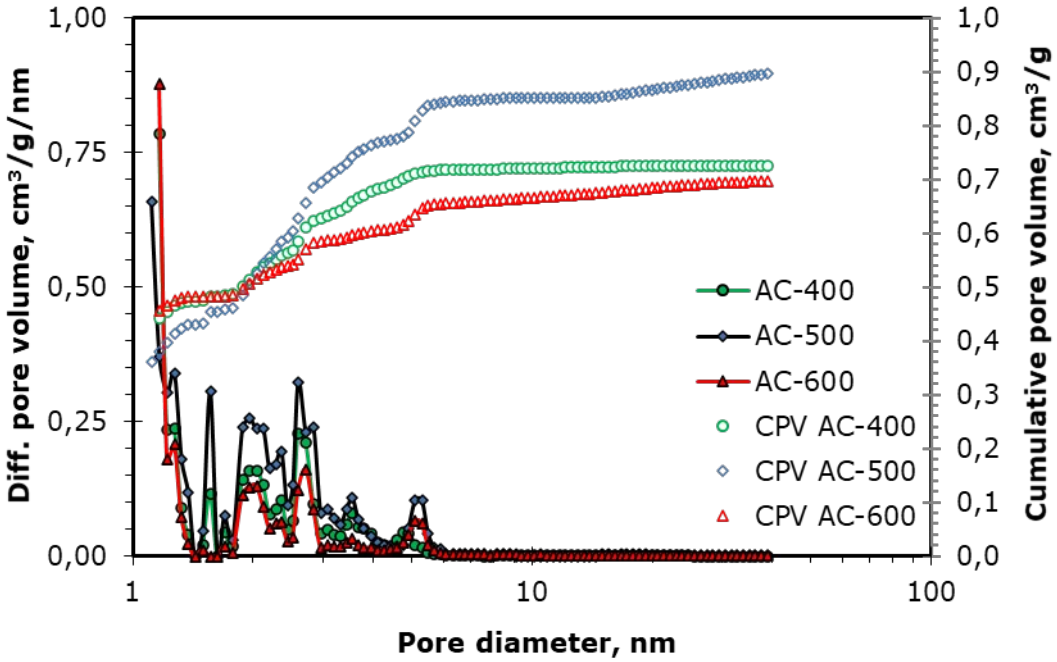

Figure 2: Pore size distributions (NLDFT) and cumulative pore volumes of AC-400, AC500 and AC-600 (CPV: Cumulative pore volume).

Tablo 1: Surface area and ore volume values of AC-400, AC-500, and AC-600.

Sample	BET surface area, m^2/g	Total pore volume[a], cm^3/g	V_{micro}[b], cm^3/g	V_{meso}[c], cm^3/g	V_{micro}, %	V_{meso}, %
AC-400	1385	0.7688	0.5206	0.2482	67.72	32.28
AC-500	1583	0.9545	0.5152	0.4393	53.98	46.02
AC-600	1276	0.7394	0.5115	0.2279	69.18	30.82

[a] calculated at $P/P_0 = 0.99$
[b] according to NLDFT

[c] V_{meso} = Total pore volume - V_{micro}

The micropore volumes of the samples were very close to each other and it can be argued that they were not affected much by the pre-carbonisation temperature. However, there was a significant difference in mesopore volume values. While the AC-400 and AC-600 samples had close micropore and mesopore fractions, AC-500 contained the highest mesopore fraction. It was clear that microporosity was dominant for AC-400 (67.72%) and AC-600 (69.18%). On the other hand, AC-500 had a balanced pore distribution (53.98% micropores, 46.02% mesopores). The mesopore volume was almost twice as much as that of the other samples. The differences observed in the structural surface properties of the activated carbon samples due to the change in pre-carbonisation temperature were related to the surface chemistry. With the increase in pre-carbonisation temperature, the surface functional groups on the fabric surface started to break away from the structure. Therefore, it was thought that the surface properties of carbonised samples obtained by applying different pre-carbonisation temperatures showed chemical differences. The most sensitive groups to heat treatment are oxygen-containing groups and they will naturally remove from the structure in different amounts with increasing temperature. When the carbonised samples with different surface chemistry are activated with KOH, the activated carbons produced (AC-400, AC-500, and AC-600) are expected to show physically and chemically different surface behaviours. The results given in Table 1 clearly show the physical changes in the structure.

3.2. FTIR Analysis

FTIR analyses were applied to investigate the effects of pre-carbonisation process on the surface chemical properties of the AC-400, AC-500 and AC-600 samples. The type of surface functional groups can be determined by FTIR analysis. Figure 3 shows the FTIR spectra of the samples. It is seen that all samples have similar absorption peaks, but the peak intensities are different. The surface functional groups corresponding to the bands obtained were as follows. The broad peak observed in the wavenumber range 3700-3200 cm^{-1} corresponds to phenolic hydroxyl, alcohol groups or moisture-induced O − H stress vibrations absorbed into the structure. The absorption bands observed around 3000-2850 cm^{-1} indicates aliphatic C − H stretching. C = O stretching vibrations in conjugated carbonyl groups were observed as small absorption bands in the 1750-1700 cm^{-1} region (Gokce & Aktas, 2014). The absorption band at 1628 cm^{-1} is attributed to C = C stretching vibrations originating from quinone groups and/or aromatic ring.

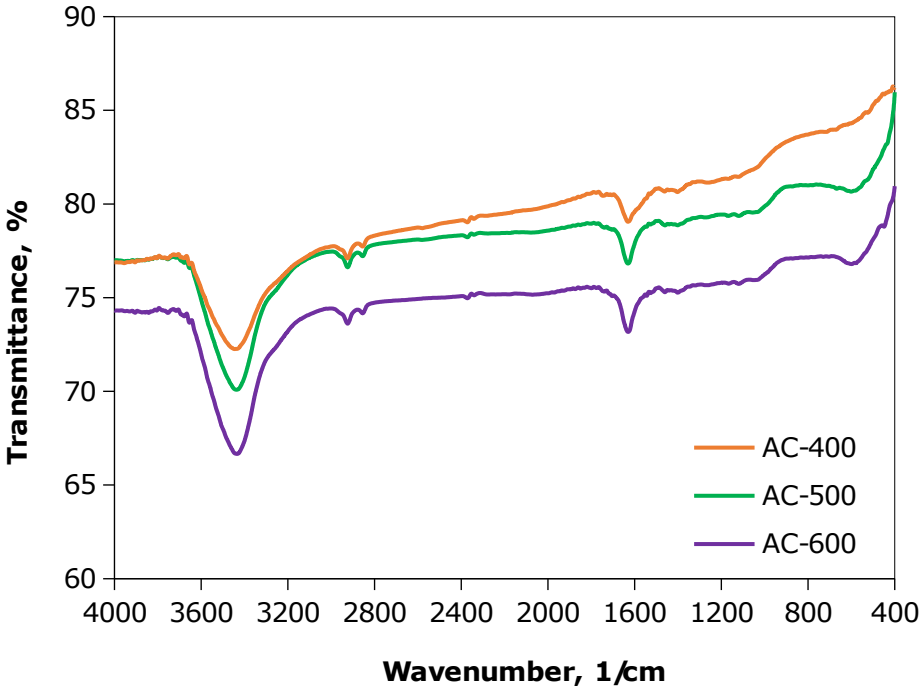

Figure 3: FTIR spectra of AC-400, AC-500 and AC-600.

The small peaks observed at 1442 cm^{-1} and 1396 cm^{-1} represents C − H deformation vibrations. In the fingerprint region (1200-700 cm^{-1}), C − O − C vibrations, aromatic CH in-plane deformation, C − O and C − C stretching vibrations or C − OH bending vibrations that may be due to hydroxyl, ether and ester structures are observed. Although the FTIR spectra did not give information about the amounts of functional groups present in the structure depending on the pre-carbonisation temperature applied, the peak intensities proved that these

groups are present in the structure in different ratios.

3.3. Contact Angle Measurements

Wettability properties of AC-400, AC-500 and AC-600 samples were determined by contact angle analysis (Figure 4). In general, samples with a contact angle below 90° have a water-loving (hydrophilic) surface. As the contact angle increases above 90°, the surface becomes water-repellent (hydrophobic). Activated carbons are amphoteric materials that contain both hydrophilic and hydrophobic surface functional groups. Polar and non-polar groups in the structures of the samples were determined by FTIR analyses. The amount of these groups directly affects the hydrophilicity or hydrophobicity of the surface. The contact angle values of AC-400, AC-500 and AC-600 samples were measured as 43.28°, 53.85° and 65.74°, respectively. The results supported the FTIR analysis. As the pre-carbonisation temperature increased from 400 °C to 600 °C, the amount of oxygen-containing functional groups removed from the structure increased.

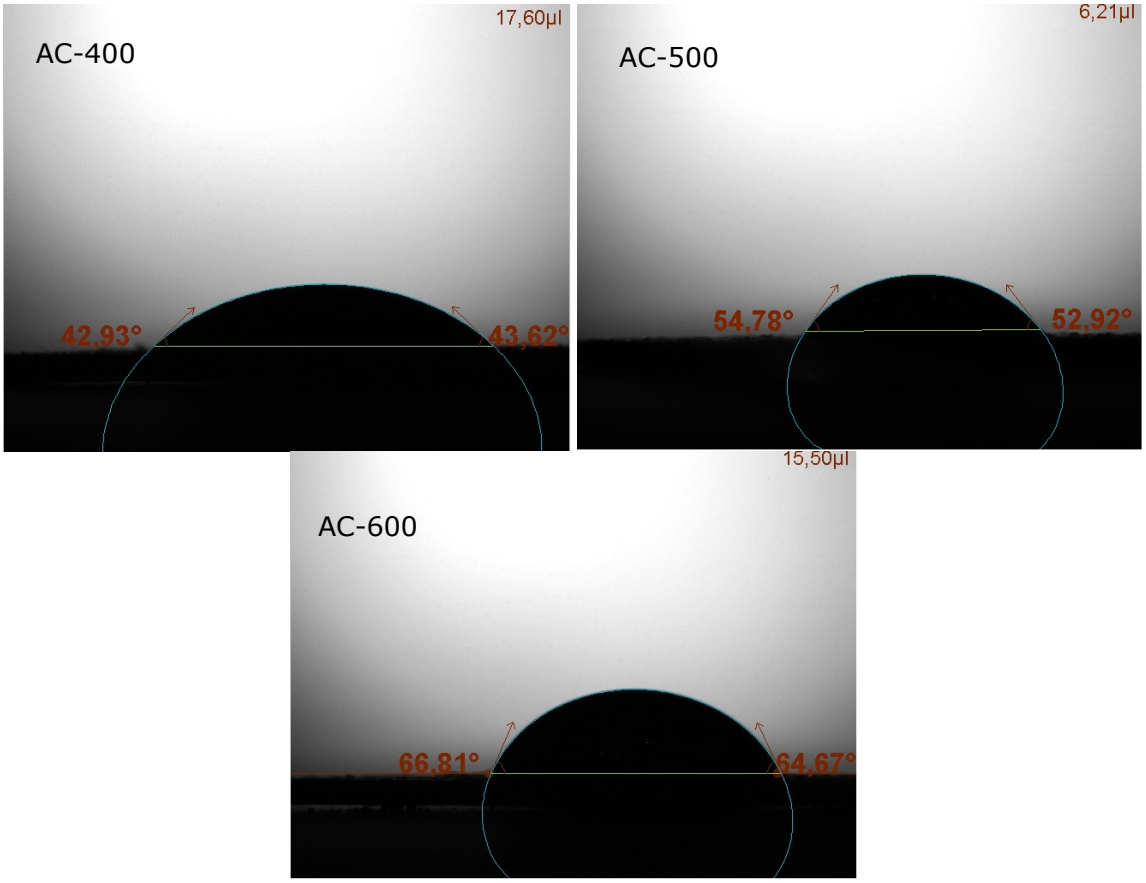

Figure 4: Contact angle measurements of AC-400, AC-500 and AC-600.

In other words, a more hydrophobic surface was formed with increasing temperature. This allowed the functional group with less oxygen content to react during activation and to form a more hydrophobic product. Contact angle measurement results also supported this phenomenon. The AC-400 had the most hydrophilic surface among the samples, while, as expected, the AC-600 was the most hydrophobic.

3.4. Adsorption Studies

The data obtained from MB adsorption experiments of the samples prepared with different pre-carbonisation processes are given in Figure 5 and Figure 6. The suitability of the adsorption data to Langmuir and Freundlich adsorption models was examined within the scope of the study. Langmuir and Freundlich adsorption models are given in Equations 1 and 2, respectively (Freundlich, 1906; Langmuir, 1918). To determine the appropriate model, appropriate curves were fitted to Equation 1 and Equation 2 with the help of SigmaPlot 12 program.

$$q_e = \frac{q_m k_L C_e}{1 + k_L C_e} \quad \text{(Eq. 1)}$$

$$q_e = k_F C_e^{\frac{1}{n}} \quad \text{(Eq. 2)}$$

Figure 5 shows the experimental adsorption data and the curves fitted according to the Langmuir model and Figure 6 shows the experimental adsorption data and the curves fitted according to the Freundlich model. The terms q_e, q_m, k_L and C_e in Equation 1 refer to equilibrium adsorption capacity, maximum monolayer adsorption capacity,

Langmuir constant and equilibrium concentration, respectively. The terms k_F and n in Equation 2 refer to the Freundlich constant and the exponent of the equation, respectively.

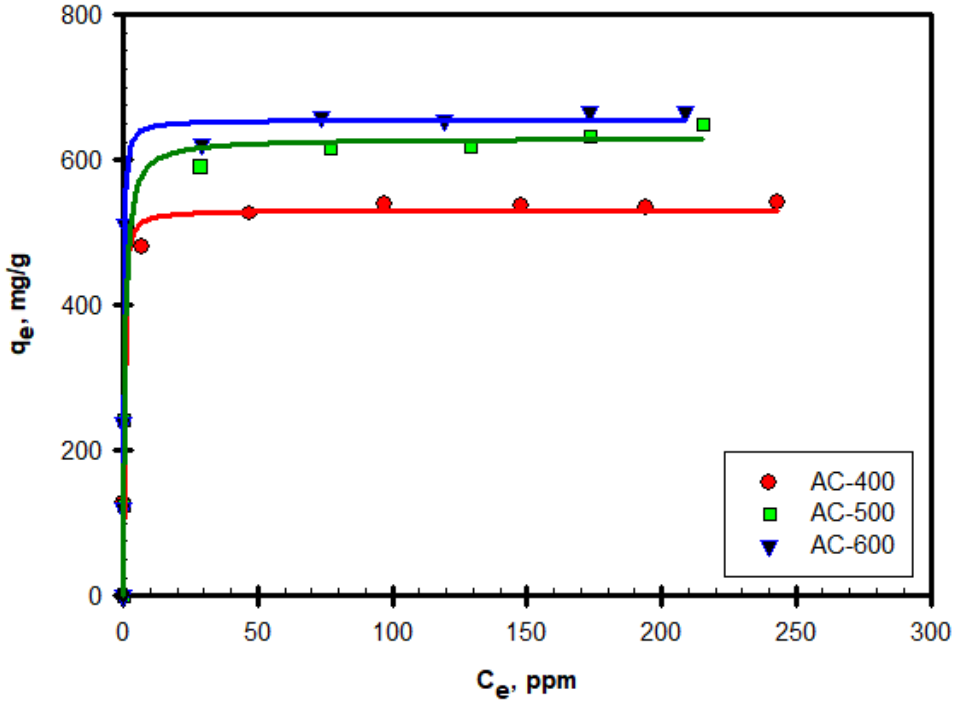

Figure 5: MB adsorption isotherms of activated carbon samples (Langmuir Adsorption Model).

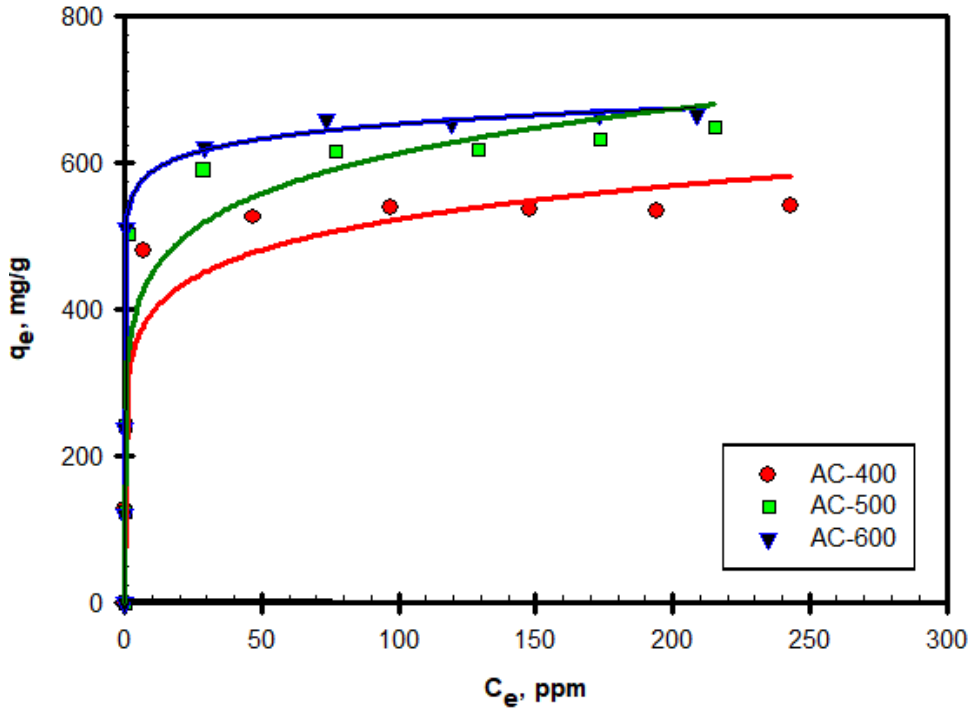

Figure 6: MB adsorption isotherms of activated carbon samples (Freundlich Adsorption Model).

The Langmuir and Freundlich model parameters calculated using the equations and adsorption data were presented in Table 2. When the R^2 values given in the table are compared, it is seen that the data fit well the Langmuir adsorption model more. Therefore, it can be said that MB is adsorbed to the surface by monolayer adsorption. The maximum monolayer adsorption capacities calculated from Langmuir adsorption model are 531.46 mg/g, 630.26 mg/g and 655.40 mg/g, respectively. It is clearly demonstrated with the help of adsorption isotherms that the change in pre-carbonisation

temperature has significant effects on adsorption performance. The highest adsorption capacity was obtained for the AC-600. Although the AC-500 had 24% higher BET surface area and 29% higher pore volume than AC-600, it exhibited lower adsorption performance. This revealed that besides physical surface properties, chemical surface properties were also important for adsorption. High surface area and mesopore structure are important parameters for dye adsorption on activated carbons. High surface area is a desirable property in activated carbons as it increases the number of potential active positions. The activated carbons should have a suitable pore opening for the dye molecules to enter the pores easily. Although the AC-500 sample had these desired properties, its lower performance against MB than AC-600 was attributed to the adsorbent-adsorbate interaction. When MB molecules diffuse into activated carbon pores, they adsorbed to certain positions on the surface. The adsorption can be through the central aromatic ring or side chain groups. It has been reported that the MB molecule may undergo molecular orientation on the activated carbon surface according to the hydrophilic/hydrophobic structure of the surface (Chalil Oglou et al., 2023). In other words, the adsorption of the molecule on the surface occurred at a certain angle depending on the number of adsorbed molecules per unit area. As the interest of the molecule to be adsorbed to the surface increases, a more regular stacking may occur.

The MB adsorption performances of the activated carbons produced within the scope of the study were compared with the performances of activated carbons similarly produced from the waste fabric and reported in Table 3. There are not many studies on the MB adsorption of activated carbons produced from the waste fabrics in available literature. When the studies in Table 3 are compared, it is seen that the highest adsorption performance was achieved with this study. All the samples performed better than the results obtained in previously published studies. It is known that the type of activation chemical used affects the activated carbon surface properties. It is thought that activated carbon produced from cotton waste fabric with KOH activation forms a more suitable surface chemistry for MB adsorption and higher adsorption performance is obtained.

Tablo 2: MB adsorption parameters of AC-400, AC-500 and AC-600.

Sample	Langmuir model			Freundlich model		
	q_m, mg/g	k_L, L/mg	R^2	n	k_F, $mg^{1-1/n}L^{1/n}/g$	R^2
AC-400	531.46	4.108	0.992	8.27	300	0.927
AC-500	630.26	1.593	0.951	7.39	328.9	0.878
AC-600	655.40	6.245	0.870	22.06	530.1	0.874

Table 3: Comparison of MB adsorption performance of activated carbons produced from textile wastes.

Raw material	Activation agent	Surface area, m^2/g	Adsorption capacity, mg/g	Reference
PET fabric	-	846	163.9	(Li et al., 2020)
Acrylic fabric	Vapour	2400	300	(You et al., 2000)
Polyester fabric	$FeCl_3$, $FeCl_2$, $FeSO_4$	1415 – 1393 – 382	445.51 – 450.23 – 149.12	(Xu et al., 2019)
Polyester fabric	$ZnCl_2$	1101.5	504	(Yu et al., 2018)
Cotton fabric	KOH	1385 – 1583 – 1276	531.46 – 630.26 – 655.40	This study

4. CONCLUSION

It was aimed to produce activated carbon samples to be tested in MB adsorption using waste shirt with 100% cotton content. To examine how the change in activated carbon surface properties will affect methylene blue adsorption, the pre-carbonisation temperature was changed during the production process. Activated carbons with three different surfaces were successfully produced by applying three different pre-carbonisation temperatures, and the differences in surface properties were revealed by characterisation studies. The produced activated carbon samples have suitable surface area and pore volume values for MB adsorption. The highest surface area and pore volume values were found in the AC-500 sample. However, the adsorption experiments showed that there was a strong relationship between the activated carbon surface chemical properties and MB adsorption. As the pre-carbonisation temperature increased, a more hydrophobic surface was obtained, and MB was adsorbed more on the activated carbon sample (AC-600). Although AC-600 has 24% lower surface area, it has the most suitable surface property for the MB adsorption. The high performance of this sample was associated with the adsorption of more dye molecules per unit surface area. When the findings obtained were compared with the studies in periodicals, it was revealed that the highest methylene blue adsorption performance was achieved in this study.

5. REFERENCES

Ambashta, R. D., & Sillanpää, M. (2010). Water purification using magnetic assistance: A review.

Journal of Hazardous Materials, *180*(1–3), 38–49. https://doi.org/10.1016/j.jhazmat.2010.04.105

Avcı, A., İnci, İ., & Baylan, N. (2020). Adsorption of ciprofloxacin hydrochloride on multiwall carbon nanotube. *Journal of Molecular Structure*, *1206*, 127711. https://doi.org/10.1016/j.molstruc.2020.127711

Ayranpınar, İ., Duyar, A., Göçer, S., Kozak, M., Köroğlu, E. O., & Cırık, K. (2023). Demir (II, III) Oksit (Fe3O4) Nanopartiküller Kullanılarak Tekstil Atıksularının Arıtılması. *Kahramanmaraş Sütçü İmam Üniversitesi Mühendislik Bilimleri Dergisi*, *26*(1), 1–7. https://doi.org/10.17780/ksujes.1142242

Barbero-Barrera, M. del M., Pombo, O., & Navacerrada, M. de los Á. (2016). Textile fibre waste bindered with natural hydraulic lime. *Composites Part B: Engineering*, *94*, 26–33. https://doi.org/10.1016/j.compositesb.2016.03.013

Bentchikou, L., Mechelouf, F. Z., Neggaz, F., & Mellah, A. (2017). REMOVAL OF HEXAVALENT CHROMIUM FROM WATER BY USING NATURAL BROWN CLAY. *Journal of the Turkish Chemical Society Section B: Chemical Engineering*, *2*, 43–52.

Bushra, R., Mohamad, S., Alias, Y., Jin, Y., & Ahmad, M. (2021). Current approaches and methodologies to explore the perceptive adsorption mechanism of dyes on low-cost agricultural waste: A review. *Microporous and Mesoporous Materials*, *319*, 111040. https://doi.org/10.1016/j.micromeso.2021.111040

Cao, H., Cobb, K., Yatvitskiy, M., Wolfe, M., & Shen, H. (2022). Textile and Product Development from End-of-Use Cotton Apparel: A Study to Reclaim Value from Waste. *Sustainability*, *14*(14), 8553. https://doi.org/10.3390/su14148553

Chai, W. S., Cheun, J. Y., Kumar, P. S., Mubashir, M., Majeed, Z., Banat, F., Ho, S.-H., & Show, P. L. (2021). A review on conventional and novel materials towards heavy metal adsorption in wastewater treatment application. *Journal of Cleaner Production*, *296*, 126589. https://doi.org/10.1016/j.jclepro.2021.126589

Chalil Oglou, R., Gokce, Y., Yagmur, E., & Aktas, Z. (2023). Production of demineralised high quality hierarchical activated carbon from lignite and determination of adsorption performance using methylene blue and p-nitrophenol: The role of surface functionality, accessible pore size and surface area. *Journal of Environmental Management*, *345*, 118812. https://doi.org/10.1016/j.jenvman.2023.118812

Darama, S. E., Mesci OktayY, B., & Çoruh, S. (2022). Investigation of the use of walnut shells as a natural biosorbent for zinc removal. *Kahramanmaraş Sütçü İmam Üniversitesi Mühendislik Bilimleri Dergisi*, *25*(4), 556–564. https://doi.org/10.17780/ksujes.1126719

Daud, W. M. A. W., & Ali, W. S. W. (2004). Comparison on pore development of activated carbon produced from palm shell and coconut shell. *Bioresource Technology*, *93*(1), 63–69. https://doi.org/10.1016/j.biortech.2003.09.015

Eder, S., Müller, K., Azzari, P., Arcifa, A., Peydayesh, M., & Nyström, L. (2021). Mass Transfer Mechanism and Equilibrium Modelling of Hydroxytyrosol Adsorption on Olive Pit–Derived Activated Carbon. *Chemical Engineering Journal*, *404*, 126519. https://doi.org/10.1016/j.cej.2020.126519

Freundlich, H. (1906). Adsorption in solution. *Phys Chem Soc, 40*, 1361–1368.

Gayathiri, M., Pulingam, T., Lee, K. T., & Sudesh, K. (2022). Activated carbon from biomass waste precursors: Factors affecting production and adsorption mechanism. *Chemosphere*, *294*, 133764. https://doi.org/10.1016/j.chemosphere.2022.133764

Gokce, Y., & Aktas, Z. (2014). Nitric acid modification of activated carbon produced from waste tea and adsorption of methylene blue and phenol. *Applied Surface Science*, *313*, 352–359. https://doi.org/10.1016/j.apsusc.2014.05.214

Gokce, Y., Yaglikci, S., Yagmur, E., Banford, A., & Aktas, Z. (2021). Adsorption behaviour of high performance activated carbon from demineralised low rank coal (Rawdon) for methylene blue and phenol. *Journal of Environmental Chemical Engineering*, *9*(2), 104819. https://doi.org/10.1016/j.jece.2020.104819

Gürten İnal, İ. I., Gökçe, Y., Yağmur, E., & Aktaş, Z. (2020). Nitrik asit ile modifiye edilmiş biyokütle temelli aktif karbonun süperkapasitör performansının incelenmesi. *Gazi Üniversitesi Mühendislik Mimarlık Fakültesi Dergisi*, *35*(3), 1243–1256. https://doi.org/10.17341/gazimmfd.425990

Gurten Inal, I. I., Holmes, S. M., Yagmur, E., Ermumcu, N., Banford, A., & Aktas, Z. (2018). The supercapacitor performance of hierarchical porous activated carbon electrodes synthesised from demineralised (waste) cumin plant by microwave pretreatment. *Journal of Industrial and Engineering Chemistry*, *61*, 124–132. https://doi.org/10.1016/j.jiec.2017.12.009

Jeihanipour, A., Aslanzadeh, S., Rajendran, K., Balasubramanian, G., & Taherzadeh, M. J. (2013). High-rate biogas production from waste textiles using a two-stage process. *Renewable Energy*, *52*, 128–135. https://doi.org/10.1016/j.renene.2012.10.042

Juanga-Labayen, J. P., Labayen, I. V., & Yuan, Q. (2022). A Review on Textile Recycling Practices and Challenges. *Textiles*, *2*(1), 174–188. https://doi.org/10.3390/textiles2010010

Langmuir, I. (1918). The adsorption of gases on plane surfaces of glass, mica and platinum. *Journal of the American Chemical Society*, *40*(9), 1361–1403.

Li, M., Lu, J., Li, X., Ge, M., & Li, Y. (2020). Removal of disperse dye from alcoholysis products of waste PET fabrics by nitric acid-modified activated carbon as an adsorbent: Kinetic and thermodynamic studies. *Textile Research Journal*, *90*(17–18), 2058–2069. https://doi.org/10.1177/0040517520909510

Liu, Q.-S., Zheng, T., Li, N., Wang, P., & Abulikemu, G. (2010). Modification of bamboo-based activated carbon using microwave radiation and its effects on the adsorption of methylene blue. *Applied Surface Science*, *256*(10), 3309–3315. https://doi.org/10.1016/j.apsusc.2009.12.025

Ozpinar, P., Dogan, C., Demiral, H., Morali, U., Erol, S., Samdan, C., Yildiz, D., & Demiral, I. (2022). Activated carbons prepared from hazelnut shell waste by phosphoric acid activation for supercapacitor electrode applications and comprehensive electrochemical analysis. *Renewable Energy*, *189*, 535–548. https://doi.org/10.1016/j.renene.2022.02.126

Pais, J. C., Santos, C. R. G., & Lo Presti, D. (2022). Application of textile fibres from tire recycling in asphalt mixtures. *Road Materials and Pavement Design*, *23*(10), 2353–2374. https://doi.org/10.1080/14680629.2021.1972034

Rápó, E., & Tonk, S. (2021). Factors Affecting Synthetic Dye Adsorption; Desorption Studies: A Review of Results from the Last Five Years (2017–2021). *Molecules*, *26*(17), 5419. https://doi.org/10.3390/molecules26175419

Reike, D., Hekkert, M. P., & Negro, S. O. (2023). Understanding circular economy transitions: The

case of circular textiles. *Business Strategy and the Environment*, *32*(3), 1032–1058. https://doi.org/10.1002/bse.3114

Shiklomanov, I. A. (2000). Appraisal and Assessment of World Water Resources. *Water International*, *25*(1), 11–32. https://doi.org/10.1080/02508060008686794

Shukla, A., Zhang, Y.-H., Dubey, P., Margrave, J. L., & Shukla, S. S. (2002). The role of sawdust in the removal of unwanted materials from water. *Journal of Hazardous Materials*, *95*(1–2), 137–152. https://doi.org/10.1016/S0304-3894(02)00089-4

Unnerstall, T. (2022). *Factfulness Sustainability*. Springer Berlin Heidelberg. https://doi.org/10.1007/978-3-662-65558-0

Ütebay, B., Çelik, P., & Çay, A. (2020). *Waste in Textile and Leather Sectors* (A. Körlü, Ed.). IntechOpen. https://doi.org/10.5772/intechopen.90014

Wang, C., Xiong, C., He, Y., Yang, C., Li, X., Zheng, J., & Wang, S. (2021). Facile preparation of magnetic Zr-MOF for adsorption of Pb(II) and Cr(VI) from water: Adsorption characteristics and mechanisms. *Chemical Engineering Journal*, *415*, 128923. https://doi.org/10.1016/j.cej.2021.128923

Wróbel-Iwaniec, I., Díez, N., & Gryglewicz, G. (2015). Chitosan-based highly activated carbons for hydrogen storage. *International Journal of Hydrogen Energy*, *40*(17), 5788–5796. https://doi.org/10.1016/j.ijhydene.2015.03.034

Xu, Z., Tian, D., Sun, Z., Zhang, D., Zhou, Y., Chen, W., & Deng, H. (2019). Highly porous activated carbon synthesized by pyrolysis of polyester fabric wastes with different iron salts: Pore development and adsorption behavior. *Colloids and Surfaces A: Physicochemical and Engineering Aspects*, *565*, 180–187. https://doi.org/10.1016/j.colsurfa.2019.01.007

Yaglikci, S., Gokce, Y., Yagmur, E., Banford, A., & Aktas, Z. (2021). Does high sulphur coal have the potential to produce high performance - low cost supercapacitors? *Surfaces and Interfaces*, *22*, 100899. https://doi.org/10.1016/j.surfin.2020.100899

Yang, W., & Cao, M. (2022). Study on the difference in adsorption performance of graphene oxide and carboxylated graphene oxide for Cu(II), Pb(II) respectively and mechanism analysis. *Diamond and Related Materials*, *129*, 109332. https://doi.org/10.1016/j.diamond.2022.109332

You, S. Y., Park, Y. H., & Park, C. R. (2000). Preparation and properties of activated carbon fabric from acrylic fabric waste. *Carbon*, *38*(10), 1453–1460. https://doi.org/10.1016/S0008-6223(99)00278-X

Yu, X., Wang, S., & Zhang, J. (2018). Preparation of high adsorption performance activated carbon by pyrolysis of waste polyester fabric. *Journal of Materials Science*, *53*(7), 5458–5466. https://doi.org/10.1007/s10853-017-1928-2